

Rice-Planted Area Extraction by RADARSAT Data Using Learning Vector Quantization Algorithm

Sigeru Omatu

Department of Electronics, Information, and Communication Engineering

Osaka Institute of Technology

Osaka, Japan

e-mail:omatu@rsh.oit.ac.jp

Abstract—The classification technique using the neural networks has been recently developed. We apply a neural network of Learning Vector Quantization (LVQ) to classify remote sensing data including microwave and optical sensors for estimation of a rice field. The method has capability of a nonlinear discrimination function which is determined by learning. The satellite data were observed before and after planting rice in 1999. Three RADARSAT and one SPOT/HRV data are used in Higashi-Hiroshima City, Japan. RADARSAT image has only one band data, which is difficult to extract a rice field. However, SAR back-scattering intensity in a rice field decreases from April to May and increases from May to June. Thus, three RADARSAT images from April to June are used for this study. The LVQ classification was applied to RADARSAT and SPOT data in order to evaluate rice field estimation. The results show that the true production rate of rice field estimation for RADARSAT data by using LVQ was approximately 60% compared with SPOT data. It is shown that the present method is much better compared with SAR image classification by the maximum likelihood (MLH) method.

Keywords-Remote sensing; Synthetic aperture radar; Neural networks; Learning vector quantization; Maximum likelihood method.

I. INTRODUCTION

Rice is the most important agricultural product in Japan and widely planted in wide places in Japan. A lot of manpower is still necessary to estimate rice field areas every year. Therefore, the development of a system to monitor the rice crop will be welcome. Satellite remote sensing images, such as LAND SATellite Thematic Mapper(LANDSAT TM), or Satellites Pour l'Observation de la Terre Visible High-Resolution data(SPOT HRV), has been expected to be used for estimating a rice field. However, these optical sensors hardly have been able to get necessary data at a suitable time since it may be often cloudy or rainy during the rice planting season in Japan.

On the other hand, space borne synthetic aperture radar penetrates through clouds. Thus, SAR observes a land surface under any weather condition. The back-scattering intensities of C-band SAR images, such as RADAR SATellite(RADARSAT), or European Remote-Sensing Satellite 1(ERS1)/SAR, change greatly from a non-cultivated bare soil condition before rice planting to an inundated condition just after rice planting [1]. In addition, RADARSAT images are rather sensitive to a change of rice biomass in a growing period of rice [2], [3]. Thus, rice area estimation is expected to be realized in an early stage. In previous works, the authors

attempted to estimate a rice field using RADARSAT fine-mode data in the same stage [4]. The estimation accuracy of a rice field was approximately 40% by comparing with the estimated area by SPOT multi-spectral data.

In this study, we attempt to detect a rice field from RADARSAT data using Learning Vector Quantization (LVQ) and to compare with accuracy by Maximum Likelihood (MLH) method. First, we will explain the LVQ algorithm and then we will show the test site and remote sensing data used here. After that, classification methods will be explained and experimental results and discussion. Finally, we will present the conclusion.

II. LEARNING VECTOR QUANTIZATION ALGORITHM

Vector quantization is to represent a data distribution using a set of units, which are called codebook vectors such that a distortion measure is minimized. The LVQ algorithm was proposed by Kohonen [5] in 1997 to find representative vectors among many vectors by learning. In LVQ, only the closest winning unit (using an Euclidean distance) to the current input data is moved toward it at each iteration.

We will show the principle of the LVQ in more detail in what follows. It consists of two layers which are an input layer and a competitive layer as shown in Fig. 1. In the input layer, input data with a dimension n are given. Let us denote the input vector by \mathbf{X} and neurons in the competitive layer are connected to the input vector with weights w_{ji} , $i = 1, 2, \dots, n$ and $j = 1, 2, \dots, M$ where connection weight vector is denoted by $\mathbf{W}_j = (w_{j1}, w_{j2}, \dots, w_{jn})$, $j = 1, 2, \dots, M$ and M is the number of neurons in the hidden layer. Furthermore, we denote the number of cluster by m , the iteration number by t , and total number of iteration by T .

In order to measure a distance between an input vector \mathbf{X} and a weight vector \mathbf{W}_j , we adopt a Euclidean norm given by

$$d_j = \|\mathbf{X} - \mathbf{W}_j\| = \sqrt{\sum_{i=1}^n (x_i - w_{ji})^2}. \quad (1)$$

We will search a neuron in the competitive layer, which attains the minimum distance and call it as the winning neuron denoted by c , that is,

$$d_c = \min_j d_j = \|\mathbf{X} - \mathbf{W}_c\|. \quad (2)$$

If the input vector \mathbf{X} and the winning unit c belong to the same cluster, then the weight vector \mathbf{W}_c will be moved such that it becomes nearer to \mathbf{X} , as shown in Fig. 2.

Conversely, if they do not belong the same cluster, the weight vector \mathbf{W}_c will be moved such that it becomes farther from \mathbf{X} , as shown in Fig. 3. Therefore, at an iteration t , if the input vector \mathbf{X} and cluster of c belong to the same cluster, then at the next iteration $t+1$

$$\mathbf{W}_j(t+1) = \mathbf{W}_j(t) + \alpha(t)(\mathbf{X} - \mathbf{W}_j(t)), \quad j = c \quad (3)$$

$$\mathbf{W}_j(t+1) = \mathbf{W}_j(t), \quad j \neq c. \quad (4)$$

On the other hand, at an iteration t , if the input vector \mathbf{X} and the winning unit c belong to different cluster, then at the next iteration $t+1$

$$\mathbf{W}_j(t+1) = \mathbf{W}_j(t) - \alpha(t)(\mathbf{X} - \mathbf{W}_j(t)), \quad j = c \quad (5)$$

$$\mathbf{W}_j(t+1) = \mathbf{W}_j(t), \quad j \neq c. \quad (6)$$

Initial values of weights w_{ji} are determined by using random numbers. The function $\alpha(t)$ means the learning rate and it is set as follows:

$$\alpha(t) = \alpha_0(1 - \frac{t}{T}) \quad (7)$$

where α_0 is a positive initial coefficient of $\alpha(t)$.

III. TEST SITE AND REMOTE SENSING DATA

The test area has a size of about 9.4 by 7.5 km in Higashi-Hiroshima City, Japan, centered at latitude N 34.42, longitude E 132.70. This site is located at the eastern part of Hiroshima City. Three multi-temporal RADARSAT fine-mode (F1F) images, taken on April 8, May 26, and June 19, in 1999 were used as test data. SPOT/HRV multi-spectral data taken on June 21, 1999 were used to generate a reference image for a rice field extraction. Above, three merged RADARSAT, as shown in Fig. 4; one SPOT image in a part of the test site is shown in Fig 5. The rice fields are mainly distributed in the bottom-center portion in the images. The land surface condition in the rice fields on April 8 is a non-cultivated bare soil before rice planting with rather rough soil surface. The surface condition on May 26 is an almost smooth water surface just after rice planting, and that on June 19 is a mixed condition of growing rice and water surface.

The RADARSAT raw data were processed using Vexcel SAR Processor (VSARP) and single-look power images with 6.25 meters ground resolution were generated. Then the images were filtered using median filter with 7 by 7 moving window. All RADARSAT and SPOT images were overlaid onto the topographic map with 1:25,000 scale. As RADARSAT images are much distorted by foreshortening due to topography, the Digital Elevation Model (DEM) with 50 meters spatial resolution issued by Geographical Survey Institute (GSI) of Japan was used to correct foreshortening of RADARSAT images.

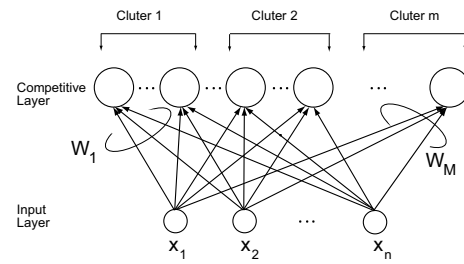


Fig. 1. LVQ structure

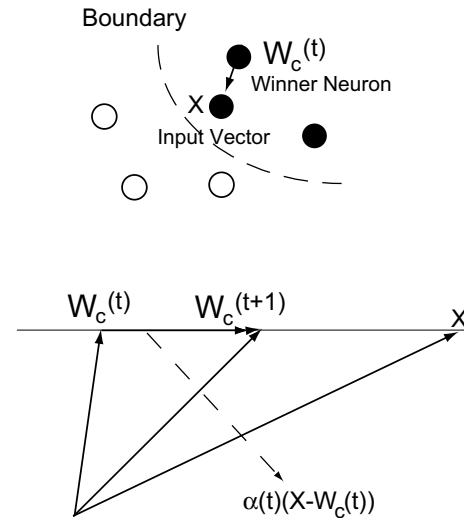


Fig. 2. LVQ learning of weights when the winning neuron belongs to the same cluster of the input \mathbf{X} where $\alpha(t) > 0$.

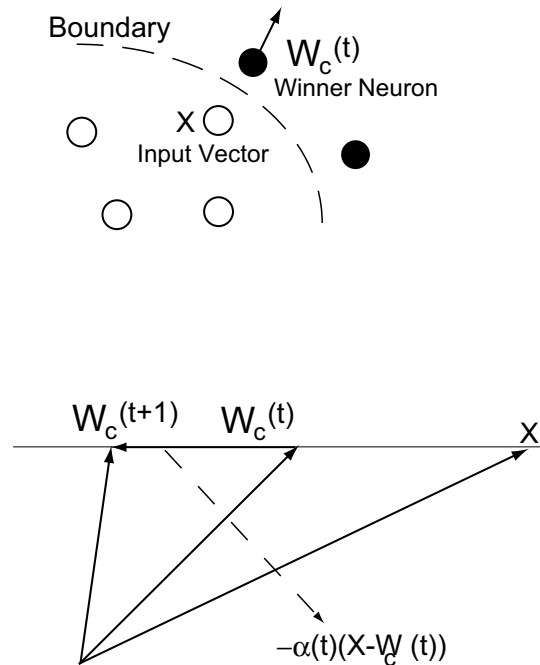


Fig. 3. LVQ learning of weights when the winning neuron belongs to the different cluster of the input \mathbf{X} where $\alpha(t) > 0$.

IV. CLASSIFICATION METHODS

Rice fields were extracted using two supervised classification methods from three temporal RADARSAT images and one SPOT image. One was an MLH classifier and the other was an LVQ classifier. In case of the LVQ classifier we adopted the initial weight $\alpha_0 = 0.05$ for RADARSAT and $\alpha_0 = 0.1$ for SPOT. The MLH classifier has been used as a land cover classification for satellite images. However, the classification results may become poor accuracy since it assumes that the distribution of each categorical data is normal distribution. Kohonen's LVQ is a classification method based on competitive neural networks, which allows us to define a group of categories on the space of input data by supervised learning algorithm.

A water region, an urban area, a rice field, and two kinds of forest were selected as target categories. We considered three sub-classes in a water region and an urban area. Furthermore, four sub-classes in a rice field and a forest. Then, we consider them as the same class. The training data for supervised classification was selected by the map and the ground truth.

As training data of SPOT image we selected as ten areas of 5x5 pixels, namely 250 pixels in each category. For the purpose of extraction of a rice field, the training data of the rice field were added 800 pixels to the data.

V. EXPERIMENTAL RESULTS AND DISCUSSION

In the beginning, SPOT image as an optical sensor classified were used for two methods of LVQ and MLH and the classification results were compared. As we can see in Tables I and II, the results of the confusion matrix were examined by SPOT data. Comparing the results of two methods, LVQ was a little better at high accuracy level, although the differences were not so large.

The results of classification rate were shown in Tables III and IV. The classification score of a rice field by SPOT was about 90 % for both of two classification methods and RADARSAT was about 80 % accuracy. Table IV shows the result by LVQ classifier of multi-temporal RADARSAT data. The results are better than MLH. In particular, the rice classification accuracy of LVQ is much better than MLH. Tables IV shows the results of average accuracy. The LVQ classifier is superior to the MLH classifier.

Figures 6 and 7 show the classified images by RADARSAT and SPOT, respectively. The rice fields were obtained by the three temporal RADARSAT images. The classification result of the urban and the forest area were different between these two images, on the other hand, water and rice areas were resembled between these two images.

We defined two indices, a True Production Rate (TPR) and a False Production Rate (FPR) for rice areas by RADARSAT. TPR is the coincidence rate of rice areas by RADARSAT within those by SPOT and FPR is the rate of non-rice areas by SPOT within rice areas by RADARSAT. As the rice area images extracted by RADARSAT are still contaminated by speckle noises, the majority filter with 7 by 7 window was applied to the rice extracted images by RADARSAT before

evaluation. The rice extracted image by SPOT was also filtered by the same majority operation as RADARSAT to make the ground resolution compatible each other, as shown in Table V.

We found experimentally that about 60 % of rice areas by SPOT were not extracted by RADARSAT and about 35 % of the areas by RADARSAT were outside areas of rice by SPOT using LVQ. This result of TPR was better than that of MLH. Figure 6 shows the results of extracted rice field in part of the test site. In the figure, the white region shows the rice field of each image. MLH has not included adjustable parameters by users compared with LVQ. The latter could more excellent results we must fine tuning parameters, especially the learning rate $\alpha(t)$ selection needs trial error to get the better results.

Figure 8 and Figure 9 show the results of extracted rice field in part of test site of RADARSAT by MLH and by the LVQ method where white color denotes rice-planted area. Figure 10 show the results of extracted rice field in part of test site of SPOT by LVQ. From these results, the classification result by LVQ becomes more detailed extraction of rice fields compared with MLH.

VI. CONCLUSIONS

A rice field extraction was attempted using multi-temporal RADARSAT data taken in the early stage of rice growing season by MLH and LVQ classifications. The LVQ classification is much better compared with classification by the MLH for a rice field extraction by RADARSAT data. However, for a quantitative evaluation, the rice field areas by RADARSAT resulted in poor coincidence rate with those by SPOT. Thus, we will apply this proposed method to other SAR data due to the extraction rice field.

ACKNOWLEDGMENT

This work was supported by JSPS KAKENHI Grant-in-Aid for Scientific Research (B) (24360141). The authors would like to thank JSPS to support this research work.

REFERENCES

- [1] Y. Suga, Y. Oguro, and S. Takeuchi, "Comparison of Various SAR Data for Vegetation Analysis over Hiroshima City", *Advanced Space Research*, vol. 23, no. 8, August, 1999, pp. 225–230.
- [2] M. Bicego and T. L. Toan, "Rice Field Mapping and Monitoring with RADARSAT Data", *International Journal of Remote Sensing*, vol. 20, no. 4, April, 1999, pp. 745–765.
- [3] S. C. Liew, and P. Chen, "Monitoring Changes in Rice Cropping System Using Space-borne SAR Imagery", *Proceedings of IGARSA'99*, October, 1999, pp. 741–743.
- [4] Y. Suga, S. Takeuchi, and Y. Oguro, "Monitoring of Rice-Planted Areas Using Space-borne SAR Data", *Proceedings of IAPRS, XXXIII, B7*, February, 2000, pp. 741–743.
- [5] T. Kohonen, "Self-Organizing Maps", Springer, 1997, pp. 206–217.

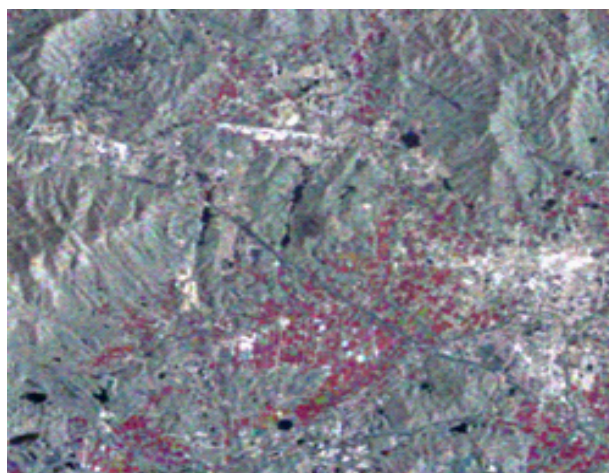


Fig. 4. RADARSAT F1F mode image in the test site.CSA & RADARSAT International 1999.



Fig. 5. SPOT-2HRV image in the test site. CNESS 1999.

TABLE I
THE CONFUSION MATRIX FOR THE CLASSIFICATION USING THE MLH(SPOT)(%)

	Water	Urban	Rice	Forest
Water	100.0	0.0	0.0	0.0
Urban	0.0	100.0	0.0	0.0
Rice	0.0	0.0	100.0	0.0
Forest	0.0	0.0	0.0	100.0

TABLE II
THE CONFUSION MATRIX FOR THE CLASSIFICATION USING THE LVQ(SPOT)(%)

	Water	Urban	Rice	Forest
Water	100.0	0.0	0.0	0.0
Urban	0.0	100.0	0.0	0.0
Rice	0.0	0.0	100.0	0.0
Forest	0.0	0.0	0.0	100.0

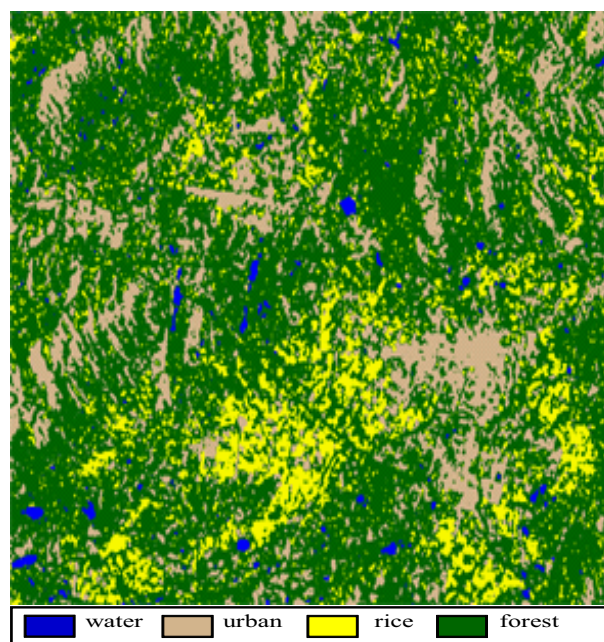


Fig. 6. Classification result of RADARSAT F1F image by LVQ.

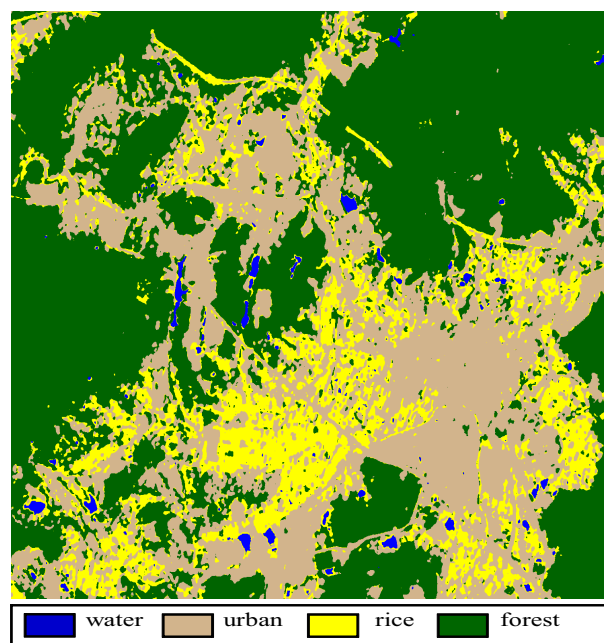


Fig. 7. Classification result of SPOT/HRV image by LVQ.

TABLE III
THE CONFUSION MATRIX FOR THE CLASSIFICATION USING THE MLH (RADARSAT) (%)

	Water	Urban	Rice	Forest
Water	100.0	0.0	0.0	0.0
Urban	0.0	62.0	0.0	38.0
Rice	0.0	4.5	53.3	42.2
Forest	2.0	3.6	9.2	85.2

TABLE IV
THE CONFUSION MATRIX FOR THE CLASSIFICATION USING THE LVQ (RADARSAT) (%)

	Water	Urban	Rice	Forest
Water	100.0	0.0	0.0	0.0
Urban	0.0	71.2	0.0	28.8
Rice	0.0	0.0	87.2	12.8
Forest	2.8	6.6	2.4	88.2

TABLE V
RESULT OF RICE FIELD EVALUATION BY RADARSAT COMPARED WITH SPOT BY LVQ. (%)

Method	TPR(%)	FPR(%)	TPR-FPR(%)
MLH	46.7	24.6	22.1
LVQ	59.1	62.0	35.6

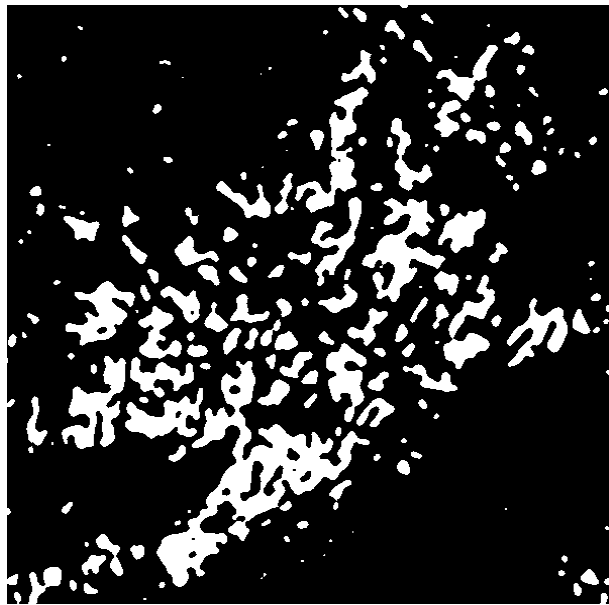


Fig. 8. Results of extracted rice field in part of test site of RADARSAT by MLH.

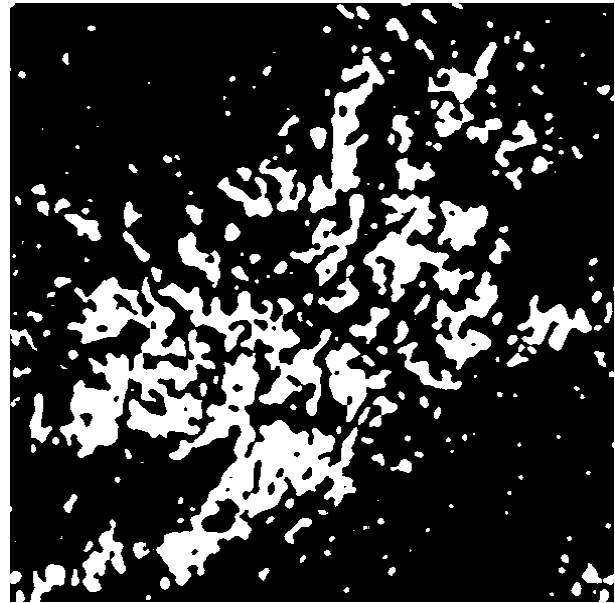


Fig. 9. Results of extracted rice field in part of test site of RADARSAT by LVQ.

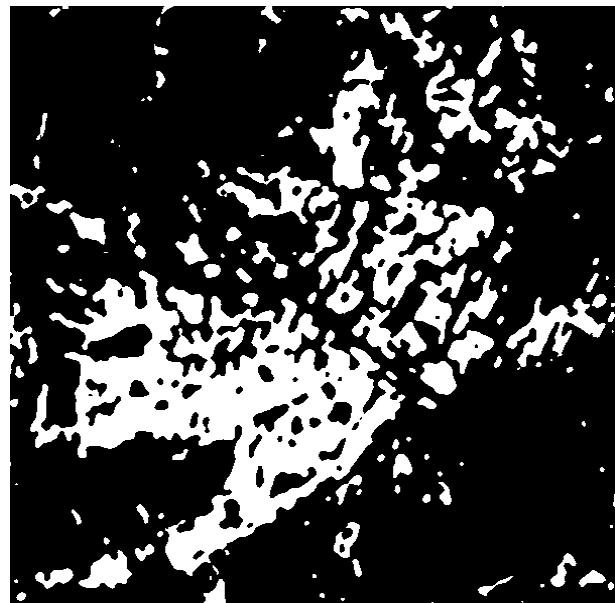


Fig. 10. Results of extracted rice field in part of test site of SPOT by LVQ.